Effect of satellite cell ablation on low-frequency-stimulated fast-to-slow fibre-type transitions in rat skeletal muscle

Karen J. B. Martins[1], Tessa Gordon[2,3], Dirk Pette[5], Walter T. Dixon[4], George R. Foxcroft[4], Ian M. MacLean[1] and Charles T. Putman[1,3]

[1] *Exercise Biochemistry Laboratory, Faculty of Physical Education and Recreation,* [2] *Division of Physical Medicine and Rehabilitation,*
[3] *The Centre for Neuroscience, Faculty of Medicine and Dentistry,* [4] *Department of Agricultural, Food and Nutritional Sciences, University of Alberta, Edmonton, AB, Canada T6G 2H9*
[5] *Department of Biology, Faculty of Science, University of Konstanz, Konstanz D-78457, Germany*

The purpose of this study was to determine whether satellite cell ablation within rat fast-twitch muscles exposed to chronic low-frequency stimulation (CLFS) would limit fast-to-slow fibre-type transitions. Twenty-nine male Wistar rats were randomly assigned to one of three groups. Satellite cells of the left tibialis anterior were ablated by weekly exposure to a 25 Gy dose of γ-irradiation during 21 days of CLFS (IRR-Stim), whilst a second group received only 21 days of CLFS (Stim). A third group received weekly doses of γ-irradiation (IRR). Non-irradiated right legs served as internal controls. Continuous infusion of 5-bromo-2′-deoxyuridine (BrdU) revealed that CLFS induced an 8.0-fold increase in satellite cell proliferation over control (mean $\pm$ S.E.M.: 23.9 $\pm$ 1.7 *versus* 3.0 $\pm$ 0.5 mm^{-2}, $P < 0.0001$) that was abolished by γ-irradiation. M-cadherin and myogenin staining were also elevated 7.7- and 3.8-fold ($P < 0.0001$), respectively, in Stim compared with control, indicating increases in quiescent and terminally differentiating satellite cells; these increases were abolished by γ-irradiation. Myonuclear content was elevated 3.3-fold ($P < 0.0001$) in Stim, but remained unchanged in IRR-Stim. Immunohistochemical analyses revealed attenuation of fast-to-slow fibre-type transitions in IRR-Stim compared with Stim. Comparable changes were observed at the protein level by SDS-PAGE. It is concluded that although considerable adaptive potential exists within myonuclei, satellite cells play a role in facilitating fast-to-slow fibre-type transitions.

(Resubmitted 9 December 2005; accepted after revision 19 January 2006; first published online 26 January 2006)
Corresponding author C. T. Putman: E-417 Van Vliet Centre, University of Alberta, Edmonton, Alberta, Canada, T6G 2H9. Email: tputman@ualberta.ca

Satellite cells are quiescent myoblasts associated with postmitotic skeletal muscle fibres that underlie the regenerative, and possibly adaptive, potential of muscle fibres. In this regard, satellite cells seem to function primarily as a source of new myonuclei by leaving their quiescent state, actively cycling, and fusing to existing skeletal muscle fibres or to each other, forming new myofibres (Bischoff, 1994; Putman *et al.* 1999*b*, 2000). The role of these muscle precursor cells during postnatal growth and regeneration is well documented (as reviewed by Schultz & McCormick, 1994; Charge & Rudnicki, 2004). The role of satellite cells in activity-induced fibre-type transitions is, however, less clear.

Slow-twitch (oxidative) skeletal muscle fibres are known to contain a larger number of myonuclei and satellite cells compared with fast-twitch (glycolytic) fibres (Gibson & Schultz, 1982, 1983). Chronic low-frequency stimulation (CLFS) is a model of muscle training that induces maximal fast-to-slow fibre-type transitions in the absence of fibre injury in rat (Simoneau & Pette, 1988; Delp & Pette, 1994; Putman *et al.* 1999*a*,*b*, 2001). These properties make the application of CLFS to rat fast-twitch muscle an ideal experimental model in which to study the contributions of satellite cells to fibre-type transitions. Our previous studies have shown that fast-to-slow fibre-type transitions are associated with increases in satellite cell activation, content and fusion to transforming fibres, especially within the IIB fibre population (Putman *et al.* 1999*b*, 2000, 2001). Collectively, these findings suggest that higher myonuclear content is a prerequisite for fast-to-slow fibre-type transitions in rat skeletal muscle, and that satellite cells play an important role in this adaptive response.

Rosenblatt and coworkers (Rosenblatt & Parry, 1992, 1993; Rosenblatt *et al.* 1994) reported that satellite cell ablation by exposure to a single 25 Gy dose of

 DOI: 10.1113/jphysiol.2005.103366

γ-irradiation prevented fibre hypertrophy but did not prevent fast-to-slow fibre-type transitions after 4 weeks of compensatory overload in rodent extensor digitorum longus muscle following removal of the synergist tibialis anterior. They concluded that satellite cell involvement was not a requirement for fibre-type transitions. That compensatory model, however, typically elicits very modest fast-to-slow fibre-type transitional stimuli compared with CLFS (Pette & Staron, 1997). Furthermore, it has been noted that a single 25 Gy dose of γ-irradiation disrupts mitotic activity of avian satellite cells in culture for only 7 days (Mozdziak *et al.* 1996) with significant recovery occurring between 9 and 12 days post-irradiation (Wakeford *et al.* 1991; McGeachie *et al.* 1993; Mozdziak *et al.* 1996). In support of these observations, studies using a rat model reported a significant increase in myotube formation 7 days after a single 20 Gy dose of ionizing irradiation (Gulati, 1987), and greater skeletal muscle DNA content 15 days after a single 25 Gy dose of ionizing irradiation (Adams *et al.* 2002). Thus the question remains as to the involvement of satellite cells in fast-to-slow fibre-type transitions.

The purpose of this study was to test the hypothesis that fast-to-slow fibre-type transitions would be attenuated in the absence of a viable satellite cell population in rat fast-twitch tibialis anterior after 21 days of CLFS. In order to sustain complete satellite cell ablation throughout 21 days of CLFS, tibialis anterior muscles were exposed to a 25 Gy dose of γ-irradiation every 7 days. A single 60 Gy dose of ionizing irradiation has been shown to not cause muscle fibre damage or abnormalities in rabbit skeletal muscle (Lewis, 1954). Likewise, the three weekly 25 Gy doses of γ-irradiation used in the present study did not cause any muscle fibre damage or abnormalities in rat skeletal muscle. Thus, this model allowed us to successfully investigate fibre-type transitions during 21 days of CLFS, in the absence of a viable satellite cell population.

Immunohistochemical detection and quantification of satellite cell content was assessed with a number of different antibodies. The calcium-dependent trans-membrane satellite cell anchor muscle (M)-cadherin was used to assess quiescent satellite cells (Kuschel *et al.* 1999; Putman *et al.* 2001). Continuous labelling with 5-bromo-2′-deoxyuridine (BrdU), followed by immuno-localization was used to detect satellite cell proliferation (Schultz, 1996), whilst the muscle-specific transcription factor myogenin was used to determine the number of satellite cell progeny committed to terminal differentiation (Putman *et al.* 1999*b*, 2000, 2001). Total myonuclear content was evaluated on serial sections stained with haematoxylin and anti-laminin (Putman *et al.* 2001). The activities of the reference enzymes citrate synthase (CS) and glyceraldehydephosphate dehydrogenase (GAPDH) were also measured to investigate coordinate changes in metabolic properties. Myosin heavy chain (MHC)-based fibre-type transitions were evaluated at the protein level by gel electrophoresis, by immunohistochemical staining of frozen serial sections with monoclonal antibodies (Putman *et al.* 1999*b*, 2000, 2001), and at the mRNA level by reverse transcriptase-polymerase chain reaction (RT-PCR) (Jaschinski *et al.* 1998; Bamford *et al.* 2003). We report that complete ablation of the satellite cell pool significantly attenuated, but did not abolish, MHC-based fast-to-slow fibre-type transitions during 21 days of CLFS.

Methods

Animals

Twenty-nine adult male Wistar rats (Charles River Laboratories, Montreal, PQ, Canada) weighing 296 ± 13.7 g (mean $\pm$ S.E.M.) were used in this study. All animal procedures were carried out in accordance with the guidelines of the Canadian Council for Animal Care and received ethical approval from the University of Alberta. Animals were individually housed under controlled environmental conditions (i.e. 22°C with alternating 12 h light and dark cycles) and received standard rat chow and water *ad libitum*. Animals were randomly assigned to one of the following three groups receiving: (1) sham operation + weekly doses of γ-irradiation focused on the left leg only (IRR, $n = 8$), (2) IRR + 21 days of CLFS of the left leg (IRR-Stim, $n = 11$), or (3) 21 days of CLFS (Stim, $n = 10$). The application of CLFS tended to elicit a compensatory effect in the contralateral control muscles due to increased weight bearing, as previously observed (Putman *et al.* 2000, 2001). Therefore, when a compensatory effect was observed, comparisons were evaluated against the right contralateral control leg of IRR (IRR-control).

Chronic low-frequency stimulation, and BrdU labelling

CLFS was applied across the left common peroneal nerve as previously described (Simoneau & Pette, 1988; Putman *et al.* 2004). Bipolar electrodes were implanted under general anaesthesia (75 mg (kg body wt)$^{-1}$ ketamine and 10 mg (kg body wt)$^{-1}$ xylazine) lateral to the common peroneal nerve of the left hindlimb, externalized at the dorsal intrascapular region, and connected to a small, portable stimulator. CLFS (10 Hz, impulse width 380 μs, 12 h day^{-1}) was applied for 21 consecutive days; strong persistent dorsiflexion was observed in the left legs of IRR-Stim and Stim twice daily throughout the study. This time point was selected because fibre-type transitions are essentially 80–90% complete after 21 days of CLFS, at both the protein and mRNA levels (Jaschinski

et al. 1998). Animals received a continuous infusion of the thymidine analogue 5-bromo-2′-deoxyuridine (BrdU, 5 mg (200 μl)$^{-1}$) via subcutaneously implanted Alzet mini-osmotic pumps (model 2004, 0.25 μl h^{-1} release rate and 200 μl volume) (Schultz, 1996).

Gamma-irradiation

On days 1, 7 and 14, animals were anaesthetized by an intraperitoneal injection of Somnotol (45 mg (kg body wt)$^{-1}$) and placed in a Gammacell 40 caesium-137 irradiation unit (Health Services Laboratory Animal Services, University of Alberta). Satellite cells of the left tibialis anterior muscle were ablated by exposing the left anterior crural compartment to a total of 25 Gy of γ-irradiation (0.56 Gy min^{-1}) (Rosenblatt *et al.* 1994), while the remainder of the animal was shielded by two 2.5 cm thick lead plates. Irradiation was interrupted at regular intervals to monitor the heart rate and respiratory rate of the animals.

Muscle sampling

Upon completion of the stimulation period, animals were killed with an overdose of Somnotol (100 mg (kg body wt)$^{-1}$), followed by exsanguination, and the tibialis anterior muscles were excised from both hindlimbs, weighed, fixed in a slightly stretched position, and frozen in melting isopentane (−159°C). Muscles were stored in liquid nitrogen (−196°C) until analysed.

Antibodies

The following monoclonal antibodies directed against adult and embryonic MHC isoforms (Schiaffino *et al.* 1988, 1989) were harvested from hybridoma cell lines obtained from the American Type Culture Collection (Manassas, VA, USA): BA-D5 (IgG, anti-MHCI), SC-71 (IgG, anti-MHCIIa), BF-F3 (IgM, anti-MHCIIb), BF-35 (IgG, not MHCIId(x)), and BF-45 (IgG, anti-MHC-embryonic). Anti-dystrophin monoclonal antibody (clone DYS2, Dy8/6C5), directed against the carboxyl terminus, was obtained from Novocastra Laboratories (Newcastle, UK). Monoclonal anti-desmin (clone DE-U-10) and monoclonal anti-vimentin (clone V9) were obtained from Sigma (Deisenhofen, Germany). Goat polyclonal anti-M-cadherin (N-19) and mouse monoclonal anti-myogenin (clone F5D) antibodies were obtained from Santa Cruz Biochemicals (Santa Cruz, CA, USA). Mouse monoclonal anti-5-bromo-2′-deoxyuridine (clone BMC 9318) was obtained from Roche Diagnostics Corporation (Indianapolis, IN, USA). Rabbit polyclonal anti-laminin (IgG) was obtained from ICN Biochemicals (Costa Mesa, CA, USA). Biotinylated horse anti-mouse IgG (rat-absorbed, affinity-purified), biotinylated horse anti-goat IgG, biotinylated goat anti-rabbit IgG, and biotinylated goat anti-mouse IgM were obtained from Vector Laboratories, Inc. (Burlingame, CA, USA). Non-specific control mouse IgG was obtained from Santa Cruz Biochemicals.

Immunohistochemistry for myosin, dystrophin, vimentin, desmin and laminin

Tibialis anterior muscles were mounted in embedding medium (Tissue-Tek OCT Compound, Miles Scientific, USA) at −20°C and 16 μm-thick frozen sections were collected from the mid-point of each muscle, also at −20°C. Immunostaining was completed according to established protocols (Putman *et al.* 2001). Briefly, sections were air-dried, washed in phosphate-buffered saline (PBS) with 0.1% (v/v) Tween-20 (PBS-T), with PBS, and then incubated for 15 min in 3% (v/v) H_2O_2 in methanol. Sections stained for MHC isoforms (i.e. BA-D5, SC-71, BF-35, BF-F3, BF-45), dystrophin, vimentin, or desmin were then incubated at room temperature for 1 h in a blocking solution (BS-1: 1% (w/v) bovine serum albumin, 10% (v/v) horse serum in PBS-T, pH 7.4) containing avidin-D blocking reagent (Vector Laboratories Inc.). Sections stained with anti-laminin or anti-MHCIIb (BF-F3) were incubated at room temperature for 1 h in a similar blocking solution, with the exception that goat serum was substituted for horse serum (BS-2). Sections were incubated overnight at 4°C with a primary antibody that was diluted in its corresponding blocking solution, also containing biotin blocking reagent (Vector Laboratories Inc.), as follows: BA-D5, 1 : 400 in BS-1; SC-71, 1 : 100 in BS-1; BF-35, 1 : 10 000 in BS-1; BF-F3, 1 : 400 in BS-2; BF-45, 1 : 50 in BS-1; DYS2, 1 : 10 in BS-1; V9, 1 : 20 in BS-1; DE-U-10, 1 : 100 in BS-1; anti-laminin, 1 : 100 in BS-2. Sections were washed as before and biotinylated horse anti-mouse IgG (BA-D5; SC-71; BF-35; BF-45; DYS2; V9; DE-U-10), biotinylated goat-anti-mouse IgM (BF-F3), or biotinylated goat anti-rabbit IgG (anti-laminin) was applied for 1 h at a dilution of 1 : 200. After several washings, sections were incubated with Vectastain ABC Reagent (i.e. avidin–biotin horseradish peroxidase (HRP) complex), according to the manufacturer's instructions (Vector Laboratories Inc.). Sections were then washed and reacted with 0.07% (w/v) diaminobenzidine, 0.05% (v/v) H_2O_2, and 0.03% (w/v) $NiCl_2$ in 50 mM Tris-HCl (pH 7.5); sections stained for desmin and laminin were reacted with the same substrate solution, but without $NiCl_2$. Control samples were run in parallel in which the primary IgM antibody was omitted, or a non-specific mouse IgG antibody was substituted (Santa Cruz). Those sections stained for laminin were counter-stained with Harris's haematoxylin (Fisher Diagnostics,

Fair Lawn, NJ, USA) and used to evaluate the total number of intrafibre myonuclei. All sections were subsequently dehydrated, cleared and mounted with Entellan (Merck, Darmstadt, Germany).

Immunohistochemistry for BrdU, myogenin and M-cadherin

Immunostaining for BrdU was completed according to Schultz, (1996), while myogenin and M-cadherin staining were completed according to our established procedures (Putman *et al.* 2000, 2001). Briefly, 16 μm-thick sections of tibialis anterior muscles were air-dried. Sections stained for BrdU were fixed for 15 min in 70% (v/v) ethanol at room temperature, whereas sections that were stained for myogenin or M-cadherin were pre-fixed for 10 min in cold acetone (−20°C). Sections were then washed in PBS-T and PBS, incubated for 15 min in 3% (v/v) H_2O_2 in methanol, and washed again. Sections stained for BrdU were further incubated in 2 M HCl for 1 h at room temperature and washed. All sections were incubated for 1 h in a blocking solution (BS-1) containing avidin-D blocking reagent (Vector Laboratories Inc.) and washed. Sections were then incubated overnight at 4°C with primary anti-BrdU (1 : 10), anti-myogenin (1 : 10), or anti-M-cadherin (1 : 50) that were diluted in BS-1, also containing biotin blocking reagent (Vector Laboratories Inc.). Sections were washed as before and biotinylated horse anti-mouse IgG (anti-BrdU; anti-myogenin) or biotinylated horse anti-goat IgG (anti-M-cadherin) was applied for 1 h at a dilution of 1 : 200. After several washings, sections were incubated with Vectastain ABC reagent. The sections were washed and reacted with diaminobenzidine (DAB), H_2O_2 and $NiCl_2$ in 50 mM Tris-HCl, pH 7.5. All sections were subsequently dehydrated, cleared and mounted with Entellan (Merck).

Immunohistochemical analyses

All semi-quantitative analyses were completed with a Leitz Diaplan microscope (Enrst Leitz Wetzlar GmbH, Germany) fitted with a Pro Series High Performance CCD camera (Media Cybernetics, USA) and a custom-designed analytical imaging program (Putman *et al.* 2000). A similar number of fibres stained for the various MHC isoforms were examined from three distinct cross-sectional areas (CSAs) of tibialis anterior (deep, middle and superficial) for each of the IRR (total fibres: 417 ± 16 fibres per muscle), IRR-Stim (total fibres: 451 ± 12 fibres per muscle), Stim (total fibres: 452 ± 35 fibres per muscle), IRR-control (total fibres: 426 ± 14 fibres per muscle), IRR-Stim contralateral control (total fibres: 404 ± 15 fibres per muscle), and Stim contralateral control (total fibres: 453 ± 35 fibres per muscle) legs. A total of 19 121 fibres were examined for fibre-type distribution analyses. Fibre cross-sectional area analyses were performed on the same fibres. Types I, IIA and IIB fibres were identified by positive staining of fibres and type IID(X) fibres were identified by the absence of staining. Fibre damage was evaluated using anti-desmin, anti-vimentin and anti-dystrophin (Putman *et al.* 1999*b*, 2001; Peters *et al.* 2003). Damaged fibres were considered to be vimentin positive, dystrophin negative, and/or to display an altered pattern of desmin staining (i.e. absence of staining or foci of positivity). The entire cross-section of each muscle was examined. The mean CSA examined for satellite cells (M-cadherin), proliferating satellite cell progeny (BrdU), terminally differentiating satellite cell progeny (myogenin), and total intrafibre myonuclei (Harris's haematoxylin with laminin) were 4.6 ± 0.04, 19.5 ± 2.1, 1.2 ± 0.1 and 1.1 ± 0.005 mm^2, respectively.

Electrophoretic analysis of myosin heavy chain protein isoforms

Quantitative MHC isoform analyses were completed according to the methods described by Hämäläinen & Pette (1996) and Putman *et al.* (2004). Muscle samples were homogenized on ice in 6 volumes of buffer containing 100 mM NaP_2O_7 (pH 8.5), 5 mM EGTA, 5 mM $MgCl_2$, 0.3 mM KCl, 10 mM DTT and 5 mg ml^{-1} of a protease inhibitor cocktail (Complete, Roche Diagnostics Corporation, Indianapolis, IN, USA). Samples were stirred for 30 min on ice and centrifuged at 12 000 *g* for 5 min at 4°C, and the supernatants were diluted 1 : 1 with glycerol. Samples were then stored at −20°C until analysed. Prior to gel loading, muscle extracts were diluted to 0.2 μg μl^{-1} in a modified Laemmli lysis buffer and boiled for 6 min. MHC isoforms were separated electrophoretically on 7% polyacrylamide gels containing glycerol, under denaturing conditions. Samples (1 μg total protein per lane) were electrophoresed in duplicate at 275 V for 24 h at 8°C. Gels were then immediately fixed and MHC isoforms were detected by silver staining and evaluated by densitometry (Syngene ChemiGenius, GeneSnap and GeneTools, Syngene, UK).

MHC mRNA analyses by reverse transcriptase-polymerase chain reaction (RT-PCR)

MHC isoform expression was further examined at the mRNA level using RT-PCR according to established procedures (Jaschinski *et al.* 1998; Bamford *et al.* 2003). The concentrations and purity of the RNA extracts were evaluated by measuring the absorbance at 260 and 280 nm using a microplate reader (Spectra Max 190, Molecular Devices, Sunnyvale, CA, USA) and 96-well flat-bottomed UV-transparent plates (Costar, Corning Incorporated Life Sciences, Acton, MA, USA). Random oligo (dT15) primers

(Invitrogen, Life Technologies, Burlington, ON, Canada) and Moloney murine leukaemia virus (M-MLV) DNA polymerase (Invitrogen, Life Technologies) were added to diluted samples (1 μg μl^{-1}) and reverse transcription was performed for 1 h at 37°C. α-Actin was used as an internal standard and its primers did not cross-react with primers for any of the MHC isoforms (Bamford *et al.* 2003). Therefore, the α-actin assay was multiplexed with each of the assays for the various MHC isoforms. The number of cDNA amplification cycles was optimized for each MHC isoform (i.e. MHCI: 25 cycles; MHCIIa: 22 cycles; MHCIId(x): 22 cycles; MHCIIb: 22 cycles). Primer sequences, annealing temperatures, and Mg^{2+} concentrations for the various primer sets have been previously described (Jaschinski *et al.* 1998; Bamford *et al.* 2003). MHCI, MHCIIa and MHCIId(x) amplicons were resolved on 2% (w/v) agarose gels for 4 h at 100 mA. MHCIIb amplicons were resolved on 4% (w/v) agarose gels, also for 4 h at 100 mA. Gels were subsequently stained for 30 min with an ethidium bromide solution, visualized under UV light, and analysed by densitometry (Syngene ChemiGenius, GeneSnap and GeneTools, Syngene, UK) (Bamford *et al.* 2003). The quantity of cDNA within each lane of the agarose gels was well within the established linear range for detection and quantification (i.e. 50 pg μl^{-1} to 10 μg μl^{-1}). All samples were normalized to the internal standard α-actin, and each MHC mRNA isoform was expressed as the percentage of total MHC mRNA. The within-sample coefficient of variation was consistently low (11 ± 1%).

Enzyme measurements

The reference enzymes citrate synthase (CS, EC 4.1.3.7) and glyceraldehyde phosphate dehydrogenase (GAPDH, EC 1.2.1.12) were extracted in a high-salt medium containing 5 mM EDTA, 100 mM sodium potassium phosphate buffer (pH 7.2) (Reichmann *et al.* 1983), with the addition of 0.1% (v/v) Triton X-100, in order to ensure complete extraction of soluble and structure-bound activities. To stabilize GAPDH, DTT was added to an aliquot of the supernatant fraction yielding a 2 mM final concentration. GAPDH activities were immediately measured at 30°C (Bass *et al.* 1969; Putman *et al.* 2004). CS activities were subsequently measured at 30°C (Srere, 1969; Putman *et al.* 2004).

Statistical analyses

Data are presented as mean ± S.E.M. Differences between group means were assessed using a two-way analysis of variance. When a significant F ratio was found, differences were located using the LSD *post hoc* analysis for planned comparisons. Differences were considered significant at $P < 0.05$; actual P values are cited.

Results

Animal and muscle weights

The animals initially weighed 296 ± 14 g and at the end of the experiment weighed 340 ± 12 g. The absolute weight gain was similar for all groups. There was no difference in weight of the tibialis anterior of IRR (691 ± 34 g) compared with IRR-control (691 ± 24 g). The weights of the tibialis anterior muscles of IRR-Stim (499 ± 30 g) and Stim (460 ± 8 g) were significantly less than their respective contralateral controls (638 ± 35 g, $P < 0.0001$ and 565 ± 20 g, $P < 0.0001$). The reduction in muscle mass in Stim and IRR-Stim was attributed to the conversion of the pure IIB fibre population to slower fibre phenotypes as opposed to a decrease in cross-sectional area (CSA) of the pure IIB fibres (Fig. 7; Table 1). This finding is consistent with our previous studies of CLFS in rat muscle (Pette & Staron, 1997; Putman *et al.* 1999*c*, 2001).

Satellite cells

Quiescent satellite cells were identified by strong positive staining for M-cadherin (Fig. 1*A*). The number of M-cadherin-positive satellite cells in the tibialis anterior of IRR did not differ from its contralateral control (Fig. 2*A*). In contrast, a 7.7-fold increase ($P < 0.00001$) was observed in Stim that was abolished in IRR-Stim (Fig. 2*A*).

Activated and previously activated satellite cells were determined by quantifying BrdU staining. Serial cross-sections of tibialis anterior muscles were analysed at ×640 magnification and only those stained nuclei that were unambiguously fused to existing muscle fibres were counted, as shown in Fig. 1*B*. Neither weekly doses of γ-irradiation (i.e. IRR 1.5 ± 0.3 positively stained nuclei mm^{-2}) nor CLFS plus IRR (i.e. IRR-Stim 1.5 ± 0.3) altered the number of activated or previously activated satellite cells compared with their respective contralateral controls (1.5 ± 0.4 and 1.2 ± 0.2). In contrast, the number of BrdU-positive nuclei of Stim was 8-fold higher ($P < 0.0001$) compared with its contralateral control (Fig. 2*B*).

Terminally differentiating satellite cell progeny were identified by strong nuclear staining for myogenin (Fig. 1*C*). The tibialis anterior of IRR (3.0 ± 0.7 myogenin-positive nuclei mm^{-2}) did not differ from its contralateral control (2.8 ± 0.6), as shown in Fig. 2*C*. In contrast, the application of CLFS in Stim resulted in a 3.8-fold increase ($P < 0.0001$) compared with its contralateral control, which was abolished in IRR-Stim.

Serial sections were also stained with anti-laminin and counterstained with haematoxylin to identify satellite cells and their progeny, as well as myonuclei (Fig. 1*D*). The number of myonuclei was calculated by subtracting the number of M-cadherin-, BrdU- and myogenin-positive

cells (Fig. 2). The number of myonuclei was not altered in IRR or IRR-Stim, but was elevated 3.3-fold in Stim ($P < 0.0001$) (Fig. 2*D*).

Structural morphology

Serial sections stained with vimentin, dystrophin, and desmin were used to identify damaged fibres (Fig. 3), as previously described (Putman *et al.* 1999*b*, 2001). The entire CSA of 58 tibialis anterior muscles were examined and only 7 fibres were vimentin-positive, dystrophin-negative and displayed foci of positivity and/or the absence of desmin staining. These 7 fibres were evenly distributed between all groups. Further inspection of haematoxylin and eosin-stained cross-sections did not reveal fibre necrosis or fibres with centrally located nuclei (Fig. 4).

Fibre-type transitions

Fibre-type transitions were assessed by semi-quantitative immunohistochemical analyses on serial sections (Fig. 5) in the deep, middle and superficial regions of each tibialis anterior muscle, in order to ensure representative sampling. Twenty-one days of CLFS induced fast-to-slow fibre-type transitions (Fig. 6). When, however, muscles were also exposed to weekly doses of γ-irradiation, fibre-type transitions were moderately attenuated. A compensatory effect was observed in the contralateral control legs of IRR-Stim and Stim, and therefore comparisons were made against IRR-control (Figs 6 and 7). When data

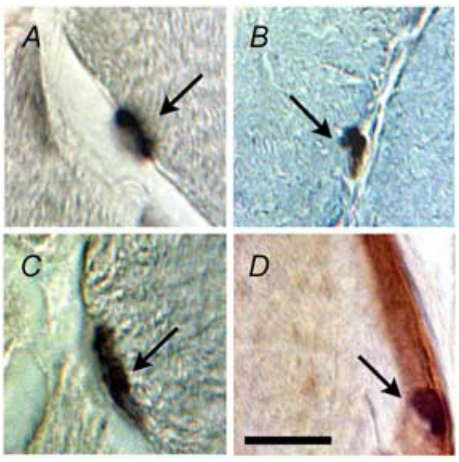

Figure 1
Photomicrographs of representative immunohistochemical stains of M-cadherin (*A*), BrdU (*B*), myogenin (*C*), and laminin and haematoxylin (*D*). These stains were used to identify satellite cells (*A*; arrow), proliferating satellite cells (*B*; arrow), terminally differentiating satellite cell progeny (*C*; arrow) and intrafibre muscle nuclei (*D*; arrow). Scale bar represents 40 μm.

Table 1. Fibre cross-sectional areas of rat tibialis anterior muscles

		Fibre cross-sectional area (μm^2)								Fibre cross-sectional area expressing a particular MHC isoform (μm^2)			
Condition	Leg	I	I/IIA	IIA	IIA/IID(X)	IIA/IID(X)/IIB	IID(X)	IID(X)/IIB	IIB	I/IIA/IID(X)/IIB	I	IIA	IID(X)	IIB
IRR	Control	818 ± 45	635 ± 191	975 ± 55	479 ± 228	—	1335 ± 71	255 ± 255	2593 ± 130	—	854 ± 57	976 ± 56	1334 ± 71	2591 ± 129
	Sham	1037 ± 123[a]	604 ± 244	1154 ± 151	550 ± 265	231 ± 231	1507 ± 152	717 ± 340	2971 ± 221	—	1019 ± 122	1152 ± 148	1498 ± 150	2938 ± 220
IRR-	Control	996 ± 89	247 ± 168	1009 ± 85	—	—	1287 ± 114	—	2564 ± 174	—	979 ± 91	1002 ± 86	1287 ± 114	2564 ± 174
Stim	Stim	1018 ± 40[a]	952 ± 227[b]	988 ± 78	592 ± 222	1563 ± 129[d]	930 ± 276[d]	204 ± 204	966 ± 345[a,b,d]	1113 ± 416	1104 ± 73[a]	1310 ± 73[a,b]	1217 ± 277	1277 ± 347[a,b,d]
Stim	Control	685 ± 34	218 ± 112	688 ± 31[a]	—	—	963 ± 43	201 ± 201	1771 ± 74[a]	—	680 ± 33	687 ± 31[a]	971 ± 46	1770 ± 74[a]
	Stim	893 ± 47[b]	558 ± 125	919 ± 79[b,d]	584 ± 176	1262 ± 121[d]	369 ± 183[a,b,c,d]	—	652 ± 166[a,b,d]	578 ± 287	889 ± 47[b,c]	1064 ± 92[b,c]	974 ± 171[d]	922 ± 202[a,b,d]

Data are means ± S.E.M. expressed as muscle fibre areas. [a]Different from IRR-control; [b]different from contralateral control; [c]different from IRR-Stim; [d]different from IRR ($P < 0.05$).

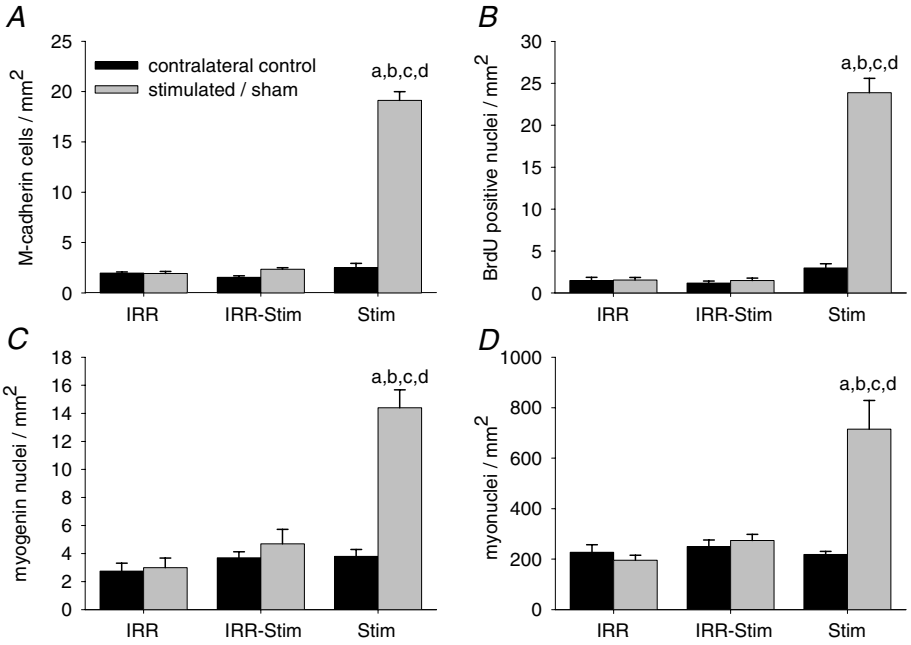

Figure 2
Number of quiescent (*A*) and proliferating (*B*) satellite cells, satellite cell progeny committed to or in the later stages of terminal differentiation (*C*), and intrafibre muscle nuclei per unit area in control and 21 day-stimulated rat tibialis anterior muscles (*D*). Statistical symbols: a, different from IRR-control; b, different from contralateral control; c, different from IRR-Stim; d, different from IRR ($P < 0.05$).

were summarized as the proportion of fibres expressing a particular MHC isoform (Fig. 6), Stim displayed increases in the percentage of fibres expressing MHCI ($P < 0.0009$) and MHCIIa ($P < 0.00001$), and decreases in the percentage of fibres expressing MHCIId(x) ($P < 0.00001$) and MHCIIb ($P < 0.00001$) compared with IRR-control. In contrast, the percentage of fibres expressing MHCI ($P < 0.04$) and MHCIIb ($P < 0.05$) in IRR-Stim differed from Stim. When, however, individual fibre types were investigated, a more obvious

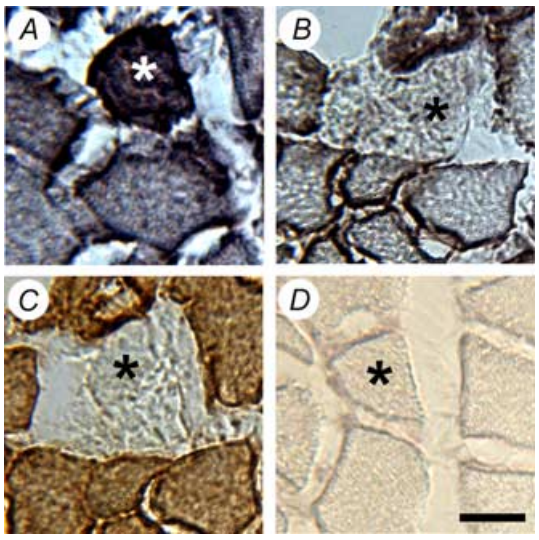

Figure 3
Example of a damaged fibre (asterisk), which was determined by positive staining for vimentin (*A*), the absence of dystrophin (*B*), and the absence of desmin positivity (*C*). *D*, IgG control. Scale bar represents 30 μm.

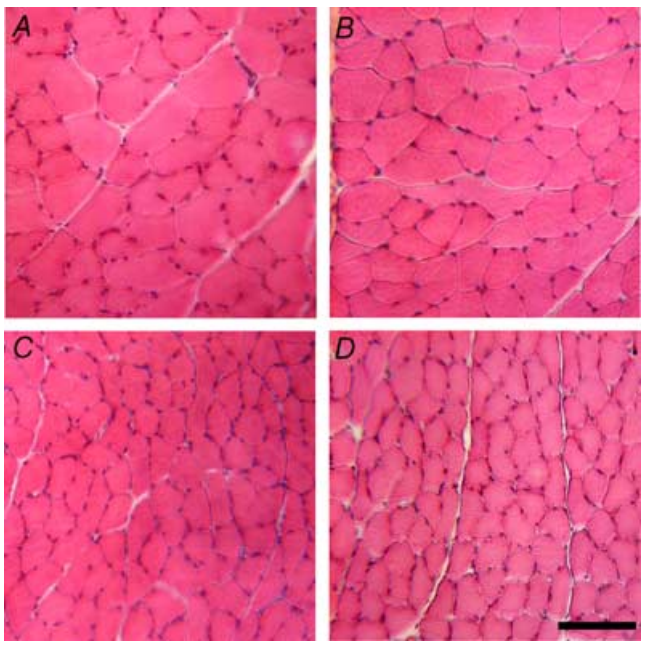

Figure 4
Representative photomicrographs of haematoxylin and eosin stains of IRR-control (*A*), IRR (*B*), IRR-Stim (*C*) and Stim (*D*). Note the absence of regenerating fibres, i.e. small fibres with centrally located nuclei. Scale bar represents 100 μm.

and detailed pattern of attenuation was evident in IRR-Stim.

Attenuation of CLFS-induced fast-to-slow fibre-type transitions was observed in types I (Fig. 7*A*), I/IIA (Fig. 7*B*), and IIA/D(X) (Fig. 7*D*) fibres of IRR-Stim. The slightly higher hybrid type I/IIA/D(X)/B fibre content in IRR-Stim compared with Stim is also consistent with delayed fibre-type transitions (Fig. 7*I*). In the slowest type I fibres, IRR-Stim remained at control levels (i.e. IRR-control), while Stim increased 1.8-fold ($P < 0.005$) compared with IRR-control (Fig. 7*A*). In IRR-Stim, the proportion of hybrid type I/IIA fibres increased 2.4-fold but was not significant, while in Stim this population of fibres significantly increased 3.2-fold ($P < 0.04$) compared with IRR-control (Fig. 7*B*). The proportion of hybrid type IIA/D(X) fibres in IRR-Stim did not differ from IRR-control, while it significantly increased in Stim ($P < 0.005$) (Fig. 7*D*). There was a small population of type I/IIA/D(X)/B hybrid fibres in IRR-Stim and Stim that differed between these groups ($P < 0.02$) (Fig. 7*I*). The type IIA and type IIA/D(X)/B fibres similarly increased (Fig. 7*C* and *E*, respectively), whilst the type IID(X) and type IIB fibres decreased by the same amount in IRR-Stim and Stim (Fig. 7*F* and *H*, respectively). For the most part, γ-irradiation alone (i.e. IRR) did not change fibre-type distribution, the lone exception being a 1.3% increase in type IID(X)/B hybrid fibres compared with IRR-control ($P < 0.02$) (Fig. 7*G*). Embryonic MHC was not detected in extrafusal fibres.

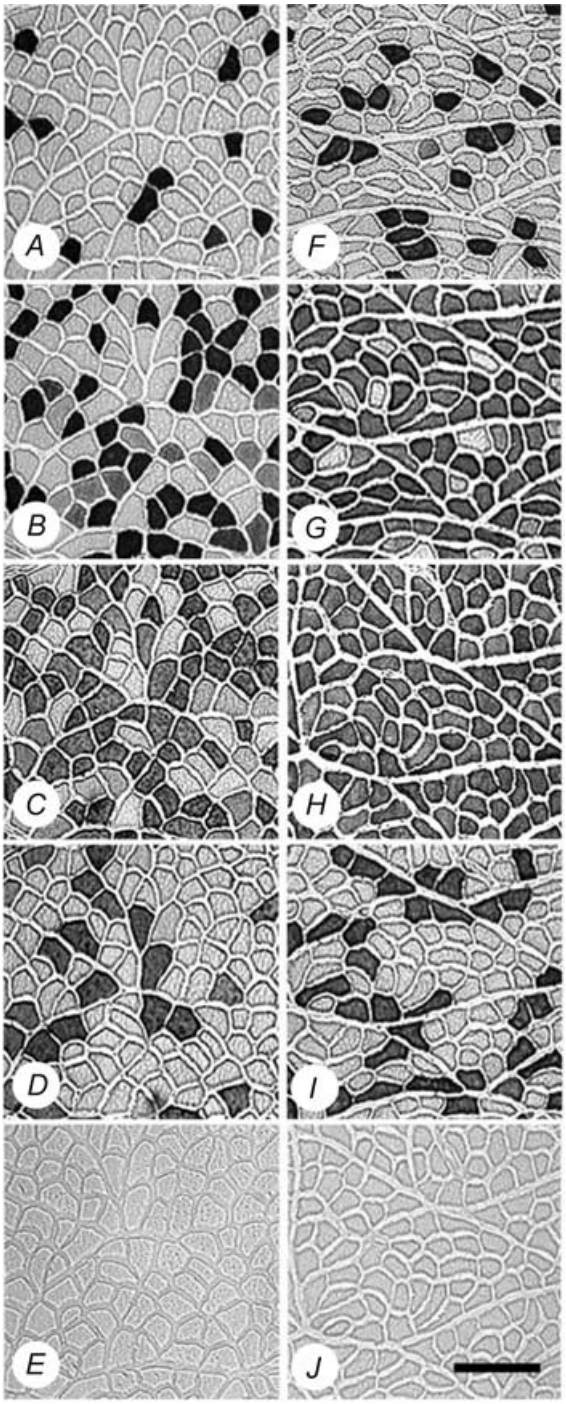

Figure 5
Representative photomicrographs of myosin heavy chain (MHC) immunohistochemistry of IRR-control (*A*, *B*, *C*, *D* and *E*) and 21 day-stimulated rat tibialis anterior muscles (*F*, *G*, *H*, *I* and *J*). *A* and *F*, immunostains for MHCI (clone BA-D5); *B* and *G*, immunostains for MHCIIa (clone SC-71); *C* and *H*, immunostains for all MHCs except MHCIId(x) (clone BF-35); *D* and *I*, immunostains for MHCIIb (clone BF-F3); *E* and *J*, IgG control. Scale bar represents 150 μm.

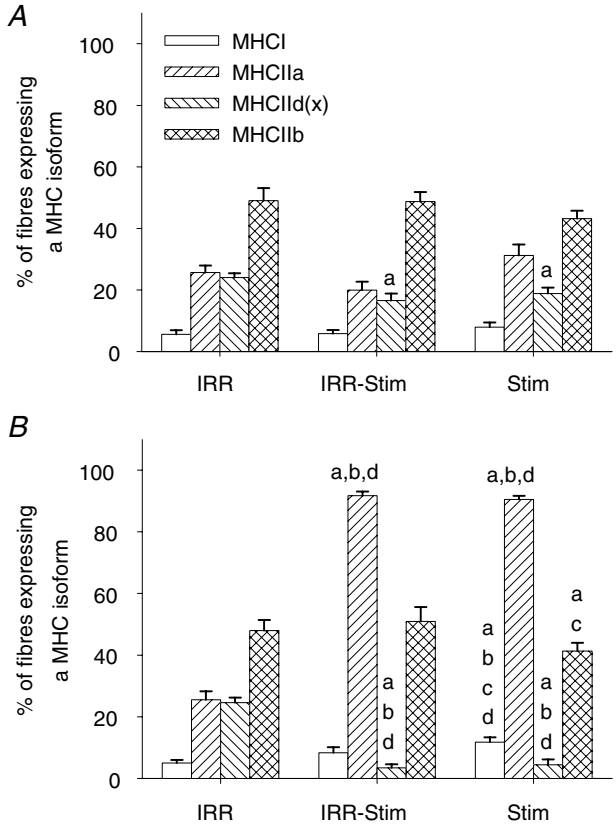

Figure 6
The percentage of fibres expressing a particular MHC isoform in contralateral control (*A*) and stimulated/sham rat tibialis anterior muscles (*B*). Statistical symbols as in Fig. 2.

MHC isoform transitions

A representative gel showing the quantitative analytical method used to measure MHC isoform content in muscle extracts is illustrated in Fig. 8. A similar MHC isoform distribution was observed between IRR and IRR-control (Fig. 9). A compensatory effect was also seen at the MHC protein level in the contralateral control legs of Stim. IRR-Stim and Stim resulted in similar MHC isoform transitions within the fast subtypes, characterized by 2.0-fold ($P < 0.00001$) decreases in MHCIIb (Fig. 9*D*) and 3.0-fold ($P < 0.00001$) increases in MHCIIa (Fig. 9*B*) compared with IRR-control. In contrast, MHCI content was 1.75-fold greater in Stim compared with IRR-control, and remained unchanged in IRR-Stim (Fig. 9*A*). MHCIId(x) content remained largely unchanged by CLFS and/or weekly exposure to γ-irradiation (Fig. 9*C*).

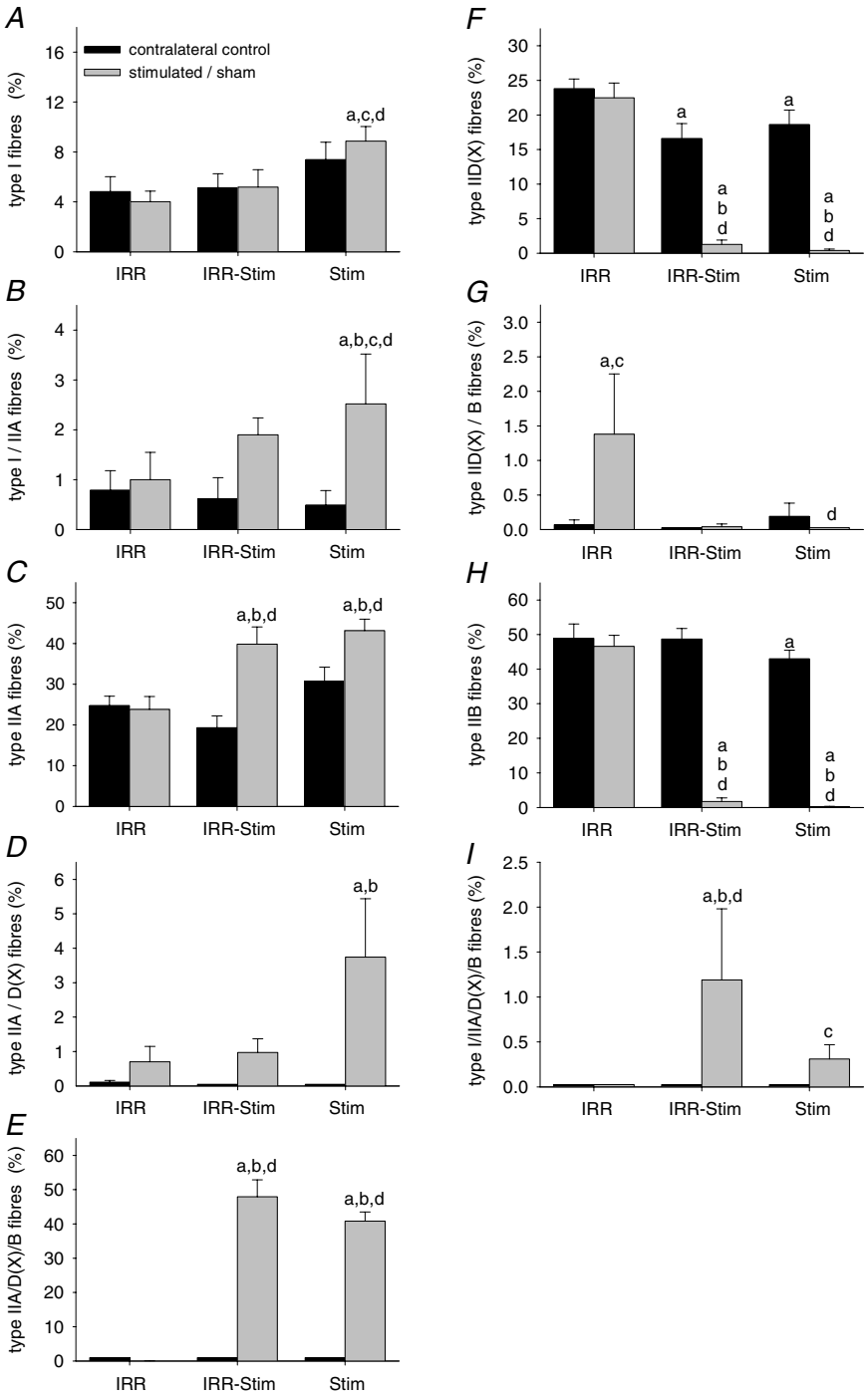

Figure 7
The proportion of pure and hybrid fibre types I (*A*), I/IIA (*B*), IIA (*C*), IIA/D(X) (*D*), IIA/D(X)/B (*E*), IID(X) (*F*), IID(X)/B (*G*), IIB(*H*) and I/IIA/D(X)/B (*I*) in rat tibialis anterior muscles. Statistical symbols as in Fig. 2.

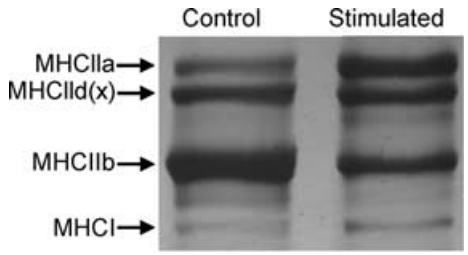

Figure 8
Example of the electrophoretic method used to quantify MHC isoform composition of rat tibialis anterior muscles. Control (IRR-control) and stimulated (Stim) are shown.

MHC mRNA expression

Examples of the semi-quantitative analytical methods used to determine mRNA expression levels of adult MHC isoforms are illustrated in Fig. 10. IRR and IRR-control displayed no differences in mRNA expression levels (i.e. MHCI, MHCIIa, MHCIId(x) and MHCIIb). Thus, irradiation alone did not cause changes in the patterns of MHC isoform expression. As observed in fibre-type and MHC protein isoform analyses, a compensatory effect was seen at the mRNA level in the contralateral control legs of IRR-Stim and Stim (Fig. 11). Twenty-one days of CLFS induced transitions in the fast-to-slow direction that were also detected at the mRNA level. MHCI mRNA levels in IRR-Stim ($P < 0.00001$) and Stim ($P < 0.00003$) were greater than IRR-control, but did not differ from one another (Fig. 11*A*). Similarly, the levels of MHCIIa mRNA in IRR-Stim ($P < 0.00001$) and Stim ($P < 0.00001$) were significantly higher than IRR-control and were also similar (Fig. 11*B*). Changes in MHCIId(x) mRNA levels were unremarkable (Fig. 11*C*). MHCIIb mRNA expression levels in IRR-Stim and Stim were significantly lower than IRR-control ($P < 0.00001$) and did not differ from one another (Fig. 11*D*).

Enzyme activities

A compensatory effect was seen in stimulated contralateral control legs (Fig. 12). Mitochondrial citrate synthase (CS) and glycolytic glyceraldehyde phosphate dehydrogenase (GAPDH) activities of IRR-Stim and Stim were equally elevated and decreased, respectively, compared with IRR-control (Fig. 12). IRR-Stim and Stim displayed greater than 2-fold increases ($P < 0.0009$) in CS activity and greater than 1.5-fold decreases ($P < 0.004$) in GAPDH activity.

Fibre cross-sectional areas

For the most part, weekly doses of γ-irradiation had no effect on fibre CSA (Table 1). When the data were summarized according to the CSA of a particular MHC isoform expressed, those fibres expressing MHCI and MHCIIa in IRR-Stim were significantly larger compared with Stim ($P < 0.03$) and IRR-control ($P < 0.02$ and $P < 0.008$, respectively). Both IRR-Stim and Stim

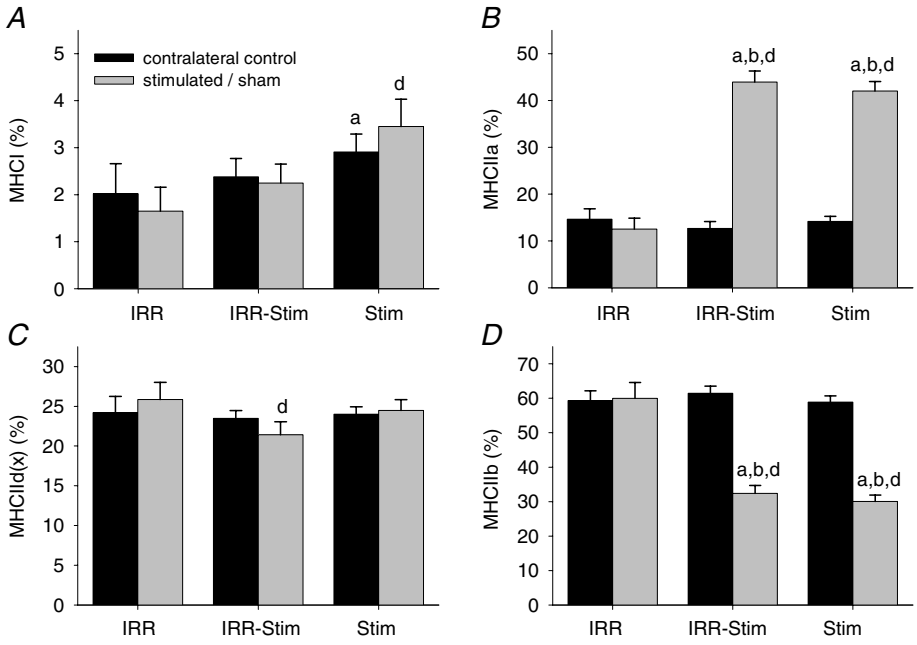

Figure 9
Percentage of MHCI (*A*), MHCIIa (*B*), MHCIId(x) (*C*) and MHCIIb (*D*) distribution as determined by densitometric evaluation of triplicate gels. Statistical symbols as in Fig. 2.

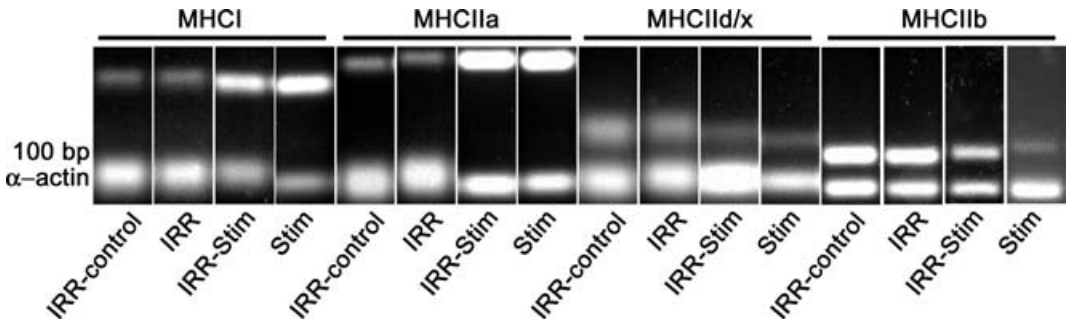

Figure 10
RT-PCR method used to evaluate mRNA expression levels of adult MHC isoforms and α-actin mRNA in the untreated right legs of IRR (IRR-control), sham-irradiated (IRR), irradiated and stimulated (IRR-Stim), and stimulated (Stim) rat tibialis anterior muscles. Sequences were amplified using a multiplex assay format for individual MHC isoforms with the internal control α-actin.

displayed similar decreases in the CSA of fibres expressing MHCIIb (2.0-fold, $P < 0.00005$ and 2.8-fold, $P < 0.00001$, respectively) compared with IRR-control. The CSA of individual fibre types varied in IRR-Stim in a manner that was consistent with attenuation of fast-to-slow fibre-type transitions. The CSA of individual fibres revealed that type I fibres of IRR-Stim were larger than IRR-control ($P < 0.05$), whereas Stim did not differ from IRR-control. Additionally, the CSA of type IID(X) fibres in IRR-Stim were 2.5-fold ($P < 0.02$) larger compared with Stim.

Discussion

The findings of the present study extend those of Rosenblatt and coworkers (Rosenblatt & Parry, 1992, 1993; Rosenblatt *et al.* 1994) and ourselves (Putman *et al.* 1999*b*, 2000, 2001). We report that exposure to three weekly doses of 25 Gy of γ-irradiation completely ablated the satellite cell population and did not cause muscle fibre damage or any structural abnormalities within the target muscle after 21 days of CLFS. This novel approach allowed us to

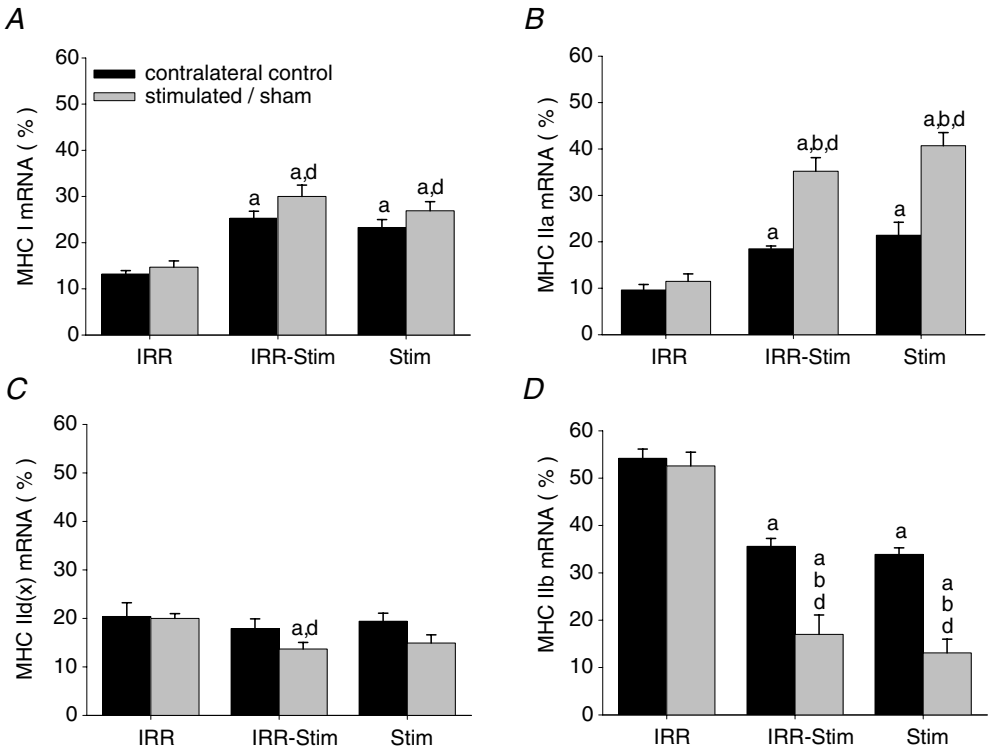

Figure 11
MHCI mRNA (*A*), MHCIIa mRNA (*B*), MHCIId(x) mRNA (*C*) and MHCIIb mRNA (*D*) expression levels expressed as the percentage of total MHC mRNA content in rat tibialis anterior muscles. Statistical symbols as in Fig. 2.

directly investigate the role of satellite cell recruitment in activity-induced fibre-type transitions, in the absence of fibre regeneration. The main finding of this study was that fast-to-slow fibre-type transitions were attenuated, but not abolished, in rat tibialis anterior muscles that were devoid of satellite cell mitotic activity.

Satellite cell ablation by irradiation

Exposure to low levels of γ-irradiation disrupts hydrogen bonds of polynucleotides causing multiple breaks in target DNA (Coggle, 1983). Once irradiated satellite cells attempt to divide, mitotic failure (Wakeford *et al.* 1991) and apoptosis (Wheldon *et al.* 1982) ensue. Post-mitotic myonuclei, on the other hand, reportedly maintain normal cellular functions after exposure to comparable levels of γ-irradiation (Wheldon *et al.* 1982; Mozdziak *et al.* 1996; Phelan & Gonyea, 1997). Previous irradiation models used to ablate skeletal muscle satellite cells have used single doses ranging from 16 to 30 Gy (Wheldon *et al.* 1982; Gulati, 1987; Mozdziak *et al.* 1996; Phelan & Gonyea, 1997; Heslop *et al.* 2000; Adams *et al.* 2002). The collective results of those studies indicate that the success of satellite cell ablation is dependent on the dose of ionizing irradiation administered, on the nature and severity of physiological stimuli leading to satellite cell activation, and on the species investigated. Although most satellite cells seem to be ablated after a single 20 to 30 Gy dose of ionizing irradiation, the basis for muscle fibre regeneration after 7 days (Gulati, 1987; Adams *et al.* 2002) appears to be the survival of a small population of radiation-resistant satellite cells (Heslop *et al.* 2000). The reason for the apparent radiation resistance of some satellite cells may include the capacity to undergo at least one mitotic division before cell death (Coggle, 1983; McGeachie *et al.* 1993; Mozdziak *et al.* 1996), the ability to recover and thus remain fusion-competent, and/or differentiated satellite cell progeny, which are past the radiosensitive phase, may fuse directly to existing fibres (Wakeford *et al.* 1991; Robertson *et al.* 1992; McGeachie *et al.* 1993; Mozdziak *et al.* 1996, 1997; Adams *et al.* 2002).

In the present study, we administered a total dose of 75 Gy over a 3 week period that may have exceeded the minimum dose required to sustain complete satellite cell ablation, including any potentially radiation-resistant satellite cells. Exposure to a 25 Gy dose of γ-irradiation each week, however, was high enough to continuously disrupt satellite cell mitotic activity, yet was low enough that it did not cause skeletal muscle damage, skeletal morphology abnormalities, or interfere with CLFS-induced changes in muscle gene expression as shown by changes in the expression of MHC isoforms, which are known to be transcriptionally regulated (Jaschinski *et al.* 1998). The absence of increases in M-cadherin- and BrdU-positive cells in IRR-Stim clearly shows that satellite cell mitosis was inhibited. Further, the absence of increases in terminally differentiating satellite cells and myonuclear content indicates that direct fusion of satellite cells to transforming muscle fibres did not occur.

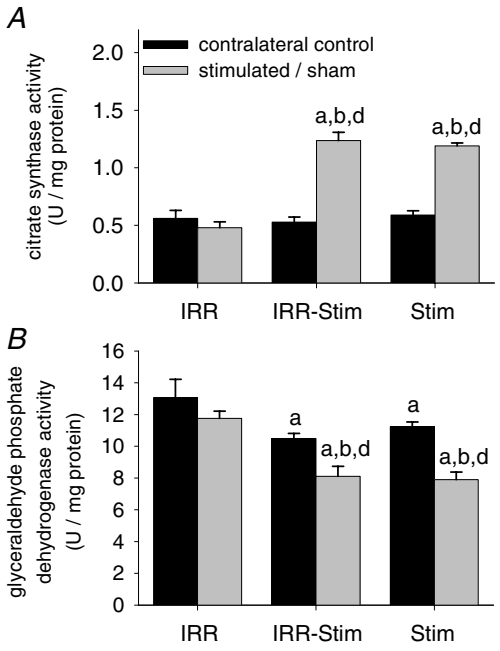

Figure 12
Citrate synthase (*A*) and glyceraldehyde phosphate dehydrogenase (*B*) activities in rat tibialis anterior muscles. Statistical symbols as in Fig. 2.

Fibre-type transitions in normal and irradiated muscles

In order to elicit a pronounced stimulus for fast-to-slow fibre-type transitions in the absence of muscle fibre regeneration, we used CLFS, a highly standardized and reproducible model of muscle training that mimics the electrical discharge pattern of slow motoneurons innervating slow-twitch muscles. As previously shown, fibre-type transitions in the fast-to-slow direction are largely restricted in low-frequency-stimulated rat muscle to transitions from type IIB to types IID(X) and IIA, whereas the transition of type IIA to type I fibres is hardly induced by CLFS in normal muscle, but greatly increases if CLFS is applied to regenerating muscle (Pette *et al.* 2002). CLFS is an ideal model for studying the effects of enhanced contractile activity on various structural, functional, metabolic and molecular properties (Pette & Vrbová, 1992, 1999; Ljubicic *et al.* 2005) because it activates all motor units of the stimulated muscle and, therefore fully challenges the adaptive potential of the target muscle (Pette & Staron, 2000). In the presence of a viable satellite cell population, CLFS is known to induce increases in satellite

cell content and activity, and large fast-to-slow phenotypic changes, specifically within the fast fibre population, which are further advanced at the mRNA level compared with protein expression levels (Jaschinski *et al.* 1998; Putman *et al.* 1999*b*, 2000, 2001). In the current study, these findings were confirmed at the nuclear, and MHC protein and mRNA levels.

Weekly doses of 25 Gy of γ-irradiation alone did not affect cellular metabolism or MHC isoform content at the protein level, which is consistent with previous findings (Wheldon *et al.* 1982; Weller *et al.* 1991; Rosenblatt & Parry, 1992, 1993). Since γ-irradiation only affected mitotically active satellite cells, any changes that occurred within γ-irradiated muscles that underwent 21 days of CLFS were due solely to the fast-to-slow fibre-type transitional stimulus mediated through existing intrafibre myonuclei.

In contrast to the work of Rosenblatt & Parry (Rosenblatt & Parry, 1992, 1993), which showed no attenuation of fast-to-slow fibre-type transitions in the extensor digitorum longus in response to 4 weeks of compensatory overload after exposure to a single dose of γ-irradiation, the results of the present study showed a modest, yet significant attenuation of CLFS-induced fast-to-slow fibre-type transitions during weekly exposure to ionizing irradiation. Detailed fibre-type analysis that included the detection of all transitional hybrid fibre types clearly showed attenuation of fibre-type transitions in the direction of IIB→I, as evidenced by the absence of stimulation-induced increases in type IIA/D(X) hybrid fibres, by the appearance of a small population of type I/IIA/IID(X)/B hybrid fibres, and by the lower proportion of type I fibres compared with Stim. These findings were also supported when data were summarized according to the percentage of fibres expressing a MHC isoform and when the same muscles were analysed by SDS-PAGE.

The absence of detectable differences in the pattern of MHC mRNA expression between IRR-Stim and Stim probably reflects the more advanced state of change at the mRNA level compared with the much slower rate of MHC protein turnover. For example, it has been reported that in rat skeletal muscle exposed to CLFS, the half-life of MHCIIb mRNA is 62 h compared with 11 days for the MHCIIb protein (Jaschinski *et al.* 1998). Our results also show that the CLFS-induced metabolic adaptations, as reflected by the similar changes in the activity levels of marker enzymes of anaerobic (GAPDH) and aerobic (CS) energy metabolism, are unaffected by satellite cell ablation. These parameters are also known to adapt more readily than contractile proteins (Pette & Vrbová, 1992; Pette & Staron, 1997). Collectively, the findings of our previous studies and the present one indicate that although considerable plasticity occurs within existing myonuclei to support fibre-type transitions, satellite cell contributions further facilitate this process.

Conclusions

The results of the present study show that CLFS-induced fast-to-slow fibre-type transitions are moderately attenuated in rat tibialis anterior muscles, in which the satellite cell population was ablated. Thus, satellite cells appear to play a direct role in fast-to-slow fibre-type transitions that is quantitative in nature. Considerable adaptive potential does, however, reside in myonuclei, which indicates that the primary role of satellite cells is to maintain the long-term stability of activity-induced fibre-type transitions.

References

Adams GR, Caiozzo VJ, Haddad F & Baldwin KM (2002). Cellular and molecular responses to increased skeletal muscle loading after irradiation. *Am J Physiol Cell Physiol* **283**, C1182–C1195.

Bamford JA, Lopaschuk GD, MacLean IM, Reinhart ML, Dixon WT & Putman CT (2003). Effects of chronic AICAR administration on metabolic and contractile phenotype in rat skeletal muscle. *Can J Physiol Pharmacol* **81**, 1072–1082.

Bass A, Brdiczka D, Eyer P, Hofer S & Pette D (1969). Metabolic differentiation of distinct muscle types at the level of enzymatic organization. *Eur J Biochem* **10**, 198–206.

Bischoff R (1994). The satellite cell and muscle regeneration. In *Myology*, ed. Engel AG & Franzini-Armstrong C, pp. 97–112. McGraw-Hill, New York.

Charge SB & Rudnicki MA (2004). Cellular and molecular regulation of muscle regeneration. *Physiol Rev* **84**, 209–238.

Coggle JE (1983). *Biological Effects of Radiation*, 2nd edn. Taylor & Francis, London.

Delp MD & Pette D (1994). Morphological changes during fiber type transitions in low-frequency-stimulated rat fast-twitch muscle. *Cell Tissue Res* **277**, 363–371.

Gibson MC & Schultz E (1982). The distribution of satellite cells and their relationship to specific fiber types in soleus and extensor digitorum longus muscles. *Anat Rec* **202**, 329–337.

Gibson MC & Schultz E (1983). Age-related differences in absolute numbers of skeletal muscle satellite cells. *Muscle Nerve* **6**, 574–580.

Gulati AK (1987). The effect of X-irradiation on skeletal muscle regeneration in the adult rat. *J Neurol Sci* **78**, 111–120.

Hämäläinen N & Pette D (1996). Slow-to-fast transitions in myosin expression of rat soleus muscle by phasic high-frequency stimulation. *FEBS Lett* **399**, 220–222.

Heslop L, Morgan JE & Partridge TA (2000). Evidence for a myogenic stem cell that is exhausted in dystrophic muscle. *J Cell Sci* **113**, 2299–2308.

Jaschinski F, Schuler MJ, Peuker H & Pette D (1998). Changes in myosin heavy chain mRNA and protein isoforms of rat muscle during forced contractile activity. *Am J Physiol Cell Physiol* **274**, C365–C370.

Kuschel R, Yablonka-Reuveni Z & Bornemann A (1999). Satellite cells on isolated myofibers from normal and denervated adult rat muscle. *J Histochem Cytochem* **47**, 1375–1383.

Lewis RB (1954). Changes in striated muscle following single intense doses of X-rays. *Lab Invest* **3**, 48–55.

Ljubicic V, Adhihetty PJ & Hood DA (2005). Application of animal models: chronic electrical stimulation-induced contractile activity. *Can J Appl Physiol* **30**, 625–643.

McGeachie JK, Grounds MD, Partridge TA & Morgan JE (1993). Age-related changes in replication of myogenic cells in mdx mice: quantitative autoradiographic studies. *J Neurol Sci* **119**, 169–179.

Mozdziak PE, Schultz E & Cassens RG (1996). The effect of in vivo and in vitro irradiation (25 Gy) on the subsequent in vitro growth of satellite cells. *Cell Tissue Res* **283**, 203–208.

Mozdziak PE, Schultz E & Cassens RG (1997). Myonuclear accretion is a major determinant of avian skeletal muscle growth. *Am J Physiol* **272**, C565–C571.

Peters D, Barash IA, Burdi M, Yuan PS, Mathew L, Friden J & Lieber RL (2003). Asynchronous functional, cellular and transcriptional changes after a bout of eccentric exercise in the rat. *J Physiol* **553**, 947–957.

Pette D, Sketelj J, Skorjanc D, Leisner E, Traub I & Bajrovic F (2002). Partial fast-to-slow conversion of regenerating rat fast-twitch muscle by chronic low-frequency stimulation. *J Muscle Res Cell Motil* **23**, 215–221.

Pette D & Staron RS (1997). Mammalian skeletal muscle fiber type transitions. *Int Rev Cytol* **170**, 143–223.

Pette D & Staron RS (2000). Myosin isoforms, muscle fiber types, and transitions. *Microsc Res Tech* **50**, 500–509.

Pette D & Vrbová G (1992). Adaptation of mammalian skeletal muscle fibers to chronic electrical stimulation. *Rev Physiol Biochem Pharmacol* **120**, 115–202.

Pette D & Vrbová G (1999). What does chronic electrical stimulation teach us about muscle plasticity? *Muscle Nerve* **22**, 666–677.

Phelan JN & Gonyea WJ (1997). Effect of radiation on satellite cell activity and protein expression in overloaded mammalian skeletal muscle. *Anat Rec* **247**, 179–188.

Putman CT, Conjard A, Peuker H & Pette D (1999*a*). Alpha-cardiac like myosin heavy chain MHCI-alpha is not upregulated in transforming rat muscle. *J Muscle Res Cell Motil* **20**, 155–162.

Putman CT, Dixon WT, Pearcey J, MacLean IM, Jendral MJ, Kiricsi M, Murdoch GK & Pette D (2004). Chronic low-frequency stimulation up-regulates uncoupling protein-3 in transforming rat fast-twitch skeletal muscle. *Am J Physiol Regul Integr Comp Physiol* **287**, R1419–R1426.

Putman CT, Düsterhöft S & Pette D (1999*b*). Changes in satellite cell content and myosin isoforms in low-frequency-stimulated fast muscle of hypothyroid rat. *J Appl Physiol* **86**, 40–51.

Putman CT, Düsterhöft S & Pette D (1999*c*). Satellite cell proliferation and myogenin expression during fast-to-slow muscle fibre type transformation. *FASEB J* **13**, A409.

Putman CT, Düsterhöft S & Pette D (2000). Satellite cell proliferation in low-frequency stimulated fast muscle of hypothyroid rat. *Am J Physiol Cell Physiol* **279**, C682–C690.

Putman CT, Sultan KR, Wassmer T, Bamford JA, Skorjanc D & Pette D (2001). Fiber-type transitions and satellite cell activation in low-frequency-stimulated muscles of young and aging rats. *J Gerontol A Biol Sci Med Sci* **56**, B510–B519.

Reichmann H, Srihari T & Pette D (1983). Ipsi- and contralateral fibre transformations by cross-reinnervation. A principle of symmetry. *Pflugers Arch* **397**, 202–208.

Robertson TA, Grounds MD & Papadimitriou JM (1992). Elucidation of aspects of murine skeletal muscle regeneration using local and whole body irradiation. *J Anat* **181**, 265–276.

Rosenblatt JD & Parry DJ (1992). Gamma irradiation prevents compensatory hypertrophy of overloaded mouse extensor digitorum longus muscle. *J Appl Physiol* **73**, 2538–2543.

Rosenblatt JD & Parry DJ (1993). Adaptation of rat extensor digitorium longus muscle to gamma irradiation and overload. *Pflugers Arch* **423**, 255–264.

Rosenblatt JD, Yong D & Parry DJ (1994). Satellite cell activity is required for hypertrophy of overloaded adult rat muscle. *Muscle Nerve* **17**, 608–613.

Schiaffino S, Gorza L, Pitton G, Saggin L, Ausoni S, Sartore S & Lomo T (1988). Embryonic and neonatal myosin heavy chain in denervated and paralyzed rat skeletal muscle. *Dev Biol* **127**, 1–11.

Schiaffino S, Gorza L, Sartore S, Saggin L, Ausoni S, Vianello M, Gundersen K & Lomo T (1989). Three myosin heavy chain isoforms in type 2 skeletal muscle fibres. *J Muscle Res Cell Motil* **10**, 197–205.

Schultz E (1996). Satellite cell proliferative compartments in growing skeletal muscles. *Dev Biol* **175**, 84–94.

Schultz E & McCormick KM (1994). Skeletal muscle satellite cells. *Rev Physiol Biochem Pharmacol* **123**, 213–257.

Simoneau J-A & Pette D (1988). Species-specific effects of chronic nerve stimulation upon tibialis anterior muscle in mouse, rat, guinea pig and rabbit. *Pflugers Arch* **412**, 86–92.

Srere PA (1969). Citrate synthase. In *Citric Acid Cycle*, ed. Lowenstein JM, pp. 3–11. Academic Press, New York, London.

Wakeford S, Watt DJ & Partridge TA (1991). X-irradiation improves mdx mouse muscle as a model of myofiber loss in DMD. *Muscle Nerve* **14**, 42–50.

Weller B, Karpati G, Lehnert S, Carpenter S, Ajdukovic B & Holland P (1991). Inhibition of myosatellite cell proliferation by gamma irradiation does not prevent the age-related increase of the number of dystrophin-positive fibers in soleus muscles of mdx female heterozygote mice. *Am J Pathol* **138**, 1497–1502.

Wheldon TE, Michalowski AS & Kirk J (1982). The effect of irradiation on function in self-renewing normal tissues with differing proliferative organisation. *Br J Radiol* **55**, 759–766.

Acknowledgements

This study was funded by research grants from the Natural Sciences and Engineering Research Council of Canada (NSERC), the Alberta Heritage Foundation for Medical Research (AHFMR), the Alberta Agricultural Research Institute, and the Canadian Institutes of Health Research. K. J. B. Martins was supported by a NSERC Post Graduate Scholarship and a Walter H. Johns Graduate Fellowship from the University of Alberta. The authors thank J. Pearcey and N. Tyreman for technical assistance. G. R. Foxcroft is supported through appointment to a Canada Research Chair in Swine Reproductive Physiology (www.chairs.gc.ca). T. Gordon is a Heritage Senior Scientist of AHFMR. C. T. Putman is a Heritage Medical Scholar of AHFMR.